Tomographic PIV study of lifted flames in turbulent Axisymmetric jets of methane.

Bertrand Lecordier[1*], Carole Gobin[1], Corine Lacour[1], Armelle Cessou[1], Benoit Tremblais[2], Lionel Thomas[3], Laurent David[3]

1: CORIA - CNRS UMR 6614 – Site Universitaire du Madrillet – BP 12 F-76821 Saint Etienne du Rouvray, France
2: Dep. XLIM-SIC - UMR CNRS 7252 - Téléport 2 – Futuroscope, France
3: INSTITUT P' - ENSMA, UPR CNRS 3346 - Téléport 2 – Futuroscope, France
Correspondent author: bertrand.lecordier@coria.fr

Abstract - In the present work, the capability of the tomo-PIV technique to measure 3D flow structures in reactive flow is evaluated in a lifted flame configuration. In combustion, two main problems can be encountered: the flame radiation and the imaging of the particle field throughout non-uniform distribution of the refractive index. In order to assess these two points, turbulent lifted flames of methane has been investigated. In that condition, the flame is detached from the burner and is in lifted-flame regime far below the blow-off condition. In this simple configuration, some parts of the methane jet is surrounded by the reaction zones and burned gases, both inducing large variations of the refractive index, which are time dependent. The main objective of this experiment is to compare the tomo-PIV results performed in reactive conditions to those obtained in the same optical arrangement without flame (free jet).

1. Introduction

Turbulent flames occur in a wide variety of domestic or industrial situations (boilers, car engines, aircraft, gas turbines…) and enhancement and optimization of combustion processes remain a major challenge in our modern societies. Over the last thirty years, one of the most effective means to provide comprehensive and detailed information of flow field, species and temperature distribution in combustion process is the use of optical diagnostics, or even their combination to measure conditioned quantities. Depending on the quantities to be measured, optical diagnostics are either adapted or specifically developed for reactive flow investigations [Kohse-Höinghaus *et al.* 2002-2005, Eckbreth, 1996]. Nowadays, the Particle Image Velocimetry (PIV) is one of the most usual ways for characterising aerodynamics in combustion systems and for investigating the interactions between the reactive zones and the structures of turbulent flows [Maurey *et al.* 2000, Cessou *et al.* 2012, Su *et al.* 2006]. Nevertheless, in more or less all configurations, these interactions are unsteady and strongly tri-dimensional and then difficult to analyse from planar 2D2C or 2D3C vector fields. The tomographic PIV seems to be a very complementary approach to 2D PIV technique to investigate such kind of complex interactions. Up to now, the tomographic PIV has been applied in cold flows and its application to reactive flow is not as straightforward as for the PIV technique. Indeed, apart from the problems of flame radiation and often the limited optical accesses in combustion devices, one of the major problems comes from the strong temperature gradient in the flow, inducing non-uniform and unsteady 3D distribution of the refractive index. The particle field is then imaged through variable optical paths depending of both flame location and burned gases regions, which can significantly affect the reconstruction step of the tomographic PIV technique. The main goal of this paper is to evaluate the effect of the temperature gradients on the tomographic PIV measurement in a simple turbulent flame configuration.

In order to investigate the feasibility to use the tomographic PIV in reactive flow, a simple configuration of lifted flames in turbulent axisymmetric jets of methane with coflowing air has been

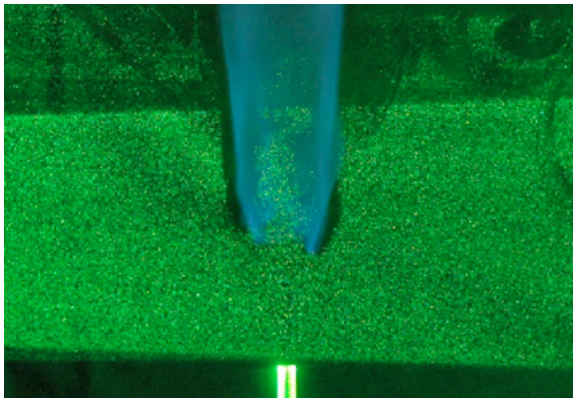

Figure 1 - Photography of the lifted flame in the light sheet with balanced seeding

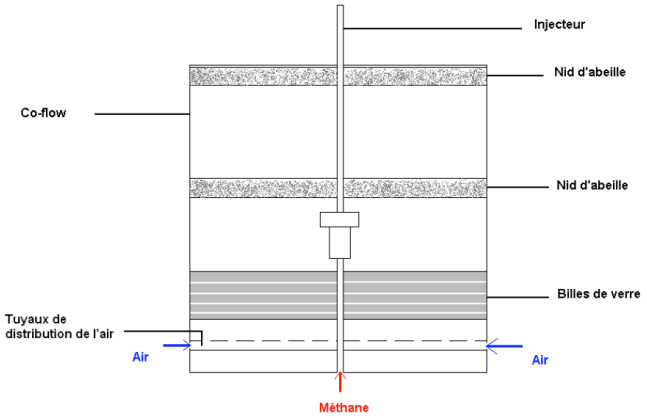

Schéma du brûleur

Figure 2 – Cross section of the burner

retained [Maurey *et al.* 2000, Cessou *et al.* 2012, Su *et al.* 2006]. For this experiment, the jet has been investigated at different Reynolds numbers varying between 3000 and 9 500. In the present paper, only one case of Reynolds number will be presented. The retained case corresponds to a flame detached from the burner in lifted-flame regime far below the blow-off condition. In that simple configuration, some parts of the methane jet is surrounded by the reaction zones and burned gases regions, both inducing large tri-dimensional variations of the refractive index, which are time dependent (see Figure 1). To evaluate the capability of the tomographic PIV technique to obtain reliable 3D velocity measurements through strong temperature gradients, the results with flame will be compared to those obtained from the same optical arrangement without flame (free jet).
The first part of the paper presents the burner and the optical arrangement of our tomographic PIV system. The second part will be focused on the description of the pre-processing of the image of particle and to the tomographic PIV algorithms. The results and discussion will be then considered in the fourth part before drawing some conclusions.

2. Experimental set-up

The burner consists of a stainless steel tube of 4 mm inner diameter of 300 mm long in order to ensure an established turbulent pipe flow for all jet velocities. The jet of methane is surrounded by a laminar low-velocity co-flow of 380 mm in diameter (cf. Figure 2). The seeding with small oil droplets of both flows can be adjusted independently. The flow rates are controlled with sonic nozzles and electronic flow meters. For the present paper, only one flow rate of the methane jet has been analysed. In that case, the flame is detached from the burner and is in lifted-flame regime far below the blow-off condition. With this burner, as shown on PIV images presented in Figure 3

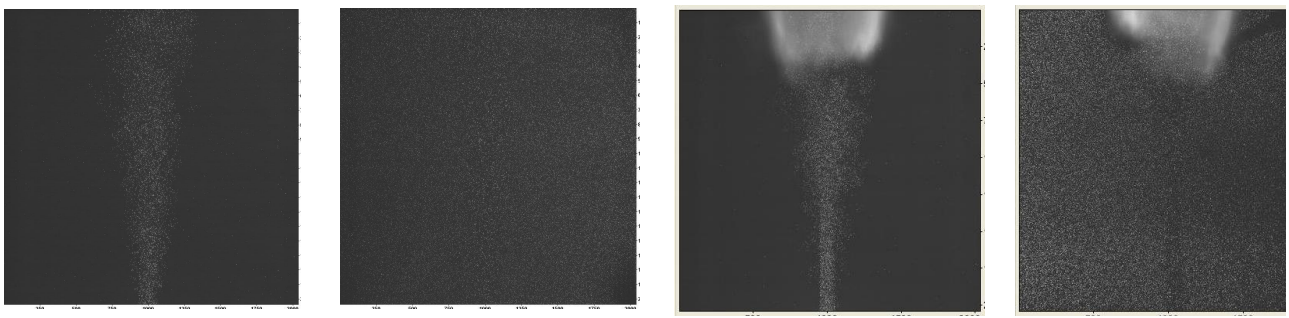

Case a) Cold flow without seeding in co-flow

Case b) Cold flow with balanced seeding

Case c) Hot flow without seeding in co-flow

Case d) Hot flow with balanced seeding

Figure 3 – Different situations of recording of the cold and hot flows

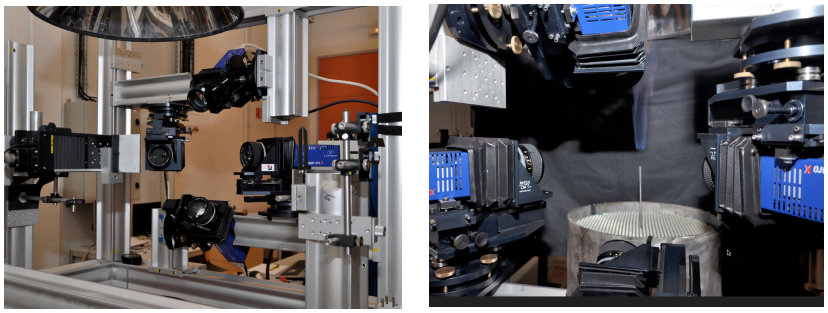

Figure 4 – Front and back views of the tomographic PIV optical arrangement and of the burner.

different configurations of seeding are possible (jet only, co-flow only or both). In the paper, only the case of balanced seeding will be presented.

For the tomo-PIV measurement, four Imager Pro X cameras of 2k.2k pixels are angularly placed at around 30° in Scheimpflug condition with a field of view of 50x50 mm2 (cf. Figure 4). The cameras are mounted with 4 Nikkor lenses of 85mm-f#1.4 with f-stop number equal to 8. Our angular optical arrangement is not the optimal one to investigate a jet configuration [Novara and Scarano 2010] and especially if investigation of flame stabilisation processes at the flame base are required to investigate the interaction of the flame with the turbulent jet. Nevertheless, in that configuration, the influence of the temperature gradient on the imaging system is maximised, in particular for the camera placed on the top. We have then favoured this configuration even if it would have been better to image the volume under the mean flame position.
The flow is lighted in volume using a dual-cavity Spectra-physics laser Nd:YAG of 400mJ@532nm. The thickness of the volume is adjustable in a range of 1 to 10 mm and is accurately bounded using a set of slits. In order to balance the recording intensities between the cameras placed in forward and backward scattering configuration, the laser light sheet is reflected in the reverse direction using a large mirror. The volume calibration is realised using a dot grid spaced of 2.5 mm, which is mounted on a motorised linear stage (NRT150). The grid has been placed at 21 positions by step of 0.5 mm over the entire thickness of the investigated volume.

3. Processing of tomo-PIV data

The computation of the 3D velocity fields have been performed from C++ programs mainly developed by PPRIME and XLIM-SIC laboratories in collaboration with CORIA and LML laboratories in the framework of a French national research program (VIVE3D). All the steps of computation, calibration, reconstruction and correlation, have been considered in the developments and are based on a C++ image-processing library (SLIP[1]). The reconstructions are performed using iterative minLOS-MART [Thomas 2010] algorithm with a correction of the calibration mapping function using a self-calibration procedure [Wieneke 2008]. For each set of data, the ten first images of the sample are used to compute the disparity maps and correct the parameters of the calibration model. Pinhole camera models are corrected iteratively (4 iterations) and the final misalignment error is less than 0.1 pixel. As explained in the following part, the images are pre-processed in order to eliminate the background. Then, a specific image processing based on a band-pass filter in spectral space is applied on the images to remove the flame radiation without affecting the particle positions. The average estimated ppp[2] on the images is equal 0.03 and so lower than the usual maximal value (ppp=0.05) when four cameras are used. The reconstruction algorithm is a minLOS-MART algorithm. The volume is initialized for each voxel using the minimum value of the corresponding pixel on each image. Only the non-zero pixels are then used to compute the MART algorithm, which leads to computation times similar to the ones obtained using the MLOS-SMART algorithm [Atkinson 2009]. Three iterations are performed, and the volume is filtered between each iteration, with a 2D Gaussian filter in the planes parallel to the laser sheet. The voxels are cubic and the volume size is 1527x1507x322 voxels. The relaxation parameter is equal to 0.7

[1] Simple Library for Image Processing: http://www.sic.sp2mi.univ-poitiers.fr/slip/
[2] Particles Per Pixel

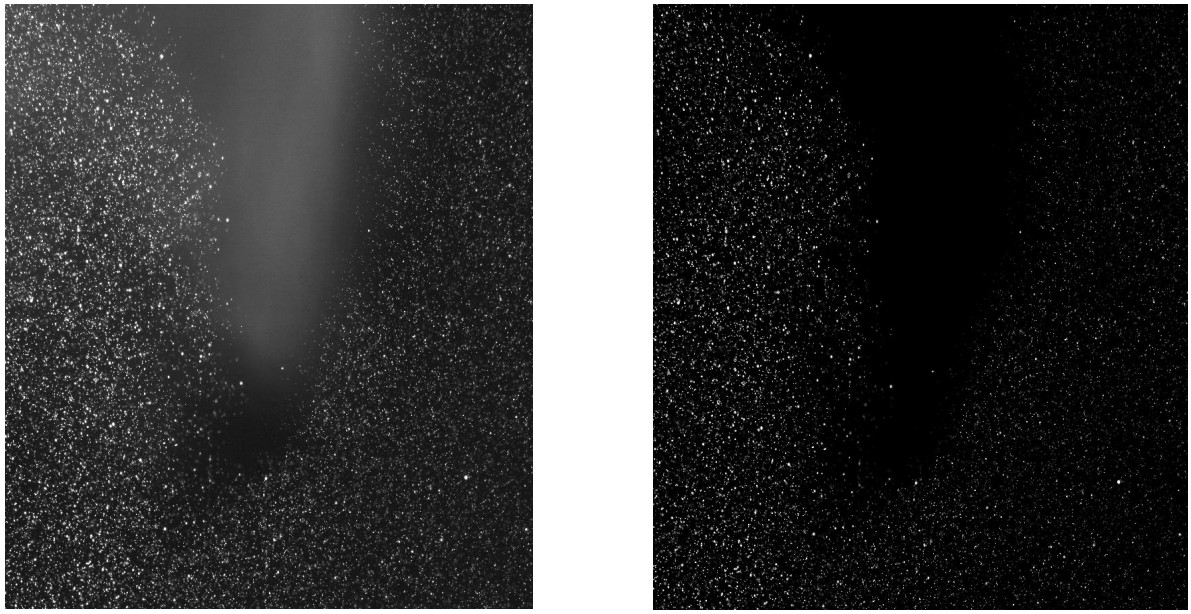

Figure 5 – Magnification of the flame region on the raw image of particle (left) and on the pre-processed image using a digital band-pass filter in the Fourier space (right).

and the re-projection quality factor Qi is always higher to 0.7, ensuring a good convergence of the algorithm. The reconstructed pairs are then analysed by means of multi-pass 3D cross-correlation of 64^3 voxels (2 mm^3) and the 3D velocity fields are validated using a median filter.

Before the reconstruction step, an important aspect to consider for reliable measurements and minimum computation load is the pre-processing of the image. Indeed for tomographic PIV, it is always better to have separate particle images superimposed to a uniform background, equal to zero. In the majority of experiments, a background subtraction followed by a Gaussian filtering is sufficient enough. In our case, the image pre-processing is trickier because on the second image of each image pair, due to a long integration time of CCD, the particle image is overlapped to the flame radiation signal (cf. Figure 3 and Figure 5). One solution to reject the flame radiation signal is to put band-pass interference filters in front of each lens. In the present experiment, this solution has not been retained for various reasons. First, in our experiment, the flame radiation is low enough to avoid any CCD saturation during the light integration time. Second, the filters induce optical aberrations and a degradation of image quality. Third, the optical transitivity is below unity and wavelength selectivity often optimised only for normal incidence, and so not fully adapted to angular arrangement. Fourth, the significant cost of high quality interference filters to equip all the cameras. In those conditions, pre-processing of image has been favoured. The flame radiation introduces a shadow on the images as shown in Figure 5, which depends on the mean flame position during the light integration period. This dependence in time is the major difficulty for using simple approaches of background correction on the instantaneous particle images. The footprint of the flame on the image being relatively smooth, a band-pass filter in the Fourier space has been retained to separate the large structures in the image and the small ones (the particles). Before the Fourier transform, the image is extended in size by duplicating image on its border to avoid jumps at the edges. Next in the Fourier space, all the frequencies below 1/25 $pixel^{-1}$ are removed with a Gaussian filtering in order to conserve only the highest frequencies. The back FFT transform provides us a new image, which only conserves the signal from the particles (cf. Figure 5) overlapped to a uniform background level, set to zero by subtraction. One example of corrected image is shown in Figure 5. The shadow image of the flame is fully suppressed even in the areas with particles. The number of particle images, their positions and their intensity distributions are not affected. In the filtered image, the burned gas regions where particles have been evaporated are

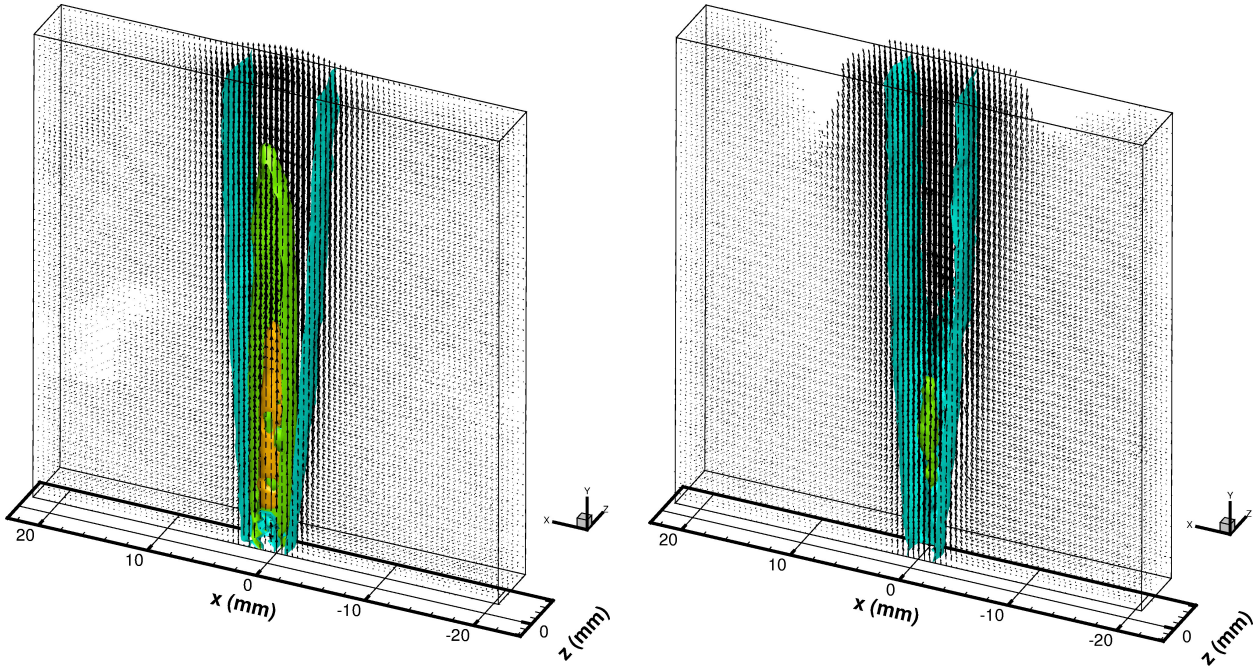

a) – Cold flow **b) – Hot-flow**

Figure 6 – Mean 3D velocity field without (a) and with (b) flame obtained from 50 instantaneous vector fields (the 3 iso-surfaces correspond to the velocities: 5, 10 and 15 m/s)

clearly observable. It should be mentioned that our filtering approach was applied in both cases, with and without combustion. In the case without combustion the FFT filtering ensures a homogeneous background level over the whole image, simple to remove by subtraction. The non-influence of filtering on the velocity measurements has been checked in the cold flow conditions.

4. Results

In the present paper, air and methane jets have been used respectively in the case without and with combustion. For each condition, 50 volumes pairs have been reconstructed and used for extracting the velocity fields. All the results have been validated and no post-processing technique is applied to the vectors fields. The number of spurious vector is always below 5% and the no-validated vectors are tagged without applying any replacement by interpolation.

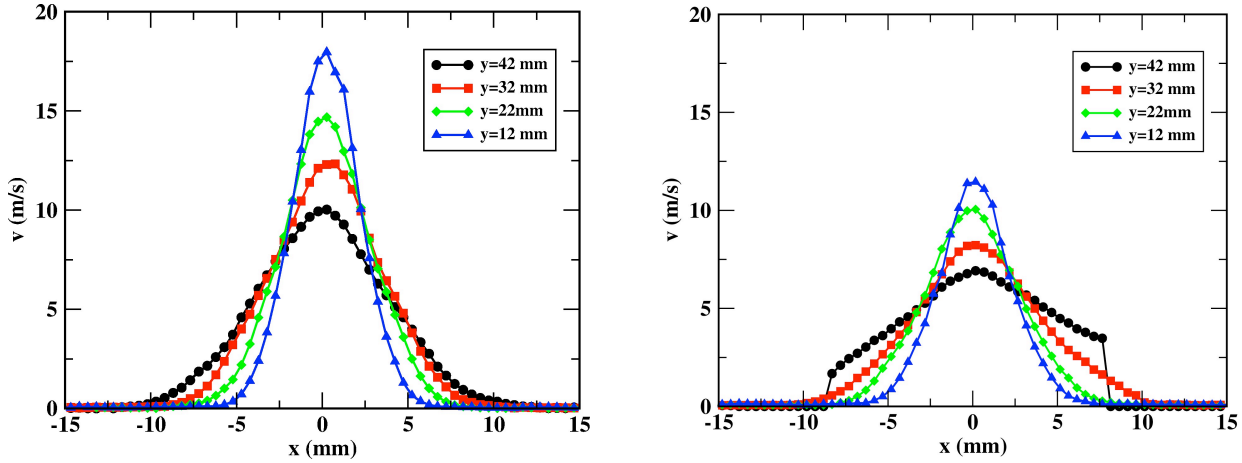

Figure 7 – Radial profiles of the mean axial velocity at different heights in the jet

The first results presented in Figure 6 show to the mean velocity fields obtained from the 50 instantaneous velocity fields. In the case without combustion (Figure 6-a), the well-known spatial development of a free turbulent jet is clearly observable with the decreasing of the axial velocity when we move away to the injector combined with a progressive spreading of the velocity profiles. The low uniform velocity of the co-flow around the jet is also correctly predicted with a measurement very close to zero considering that the time interval between volume are adapted to the velocity range of the jet. The shape and the smoothness of the iso-surface of velocity show a sufficient statistical convergence for evaluating the mean velocity from 50 instantaneous fields. In the case with combustion shown in Figure 6-b, the jet structure remains observable but with lower velocities due to a smaller velocity at the tube exit. Whether for the reconstruction or for the measurement of the mean fields, it seems that the results of tomo-PIV are not significantly affected by the presence of the flame brush and the burned gases. On the top of the jet, two symmetrical areas without vector are observable and correspond more or less to the mean location of the flame. Indeed, in the burned gases regions, the seeding particles being evaporating (cf. Figure 5), no velocity vectors are measured. On the instantaneous velocity field, those areas are fluctuating in shape and in position. To take into account the variable location of those areas in the statistics, the mean vectors are considered as statistically relevant if and only if 25 instantaneous vectors are validated at the considered position. On the mean flow field in Figure 6-b, the transition between the areas with and without vector can then be seen roughly as an indirect estimation of the mean flame position. In our experiment, a small dissymmetry on the flame position is present on the mean flow field in Figure 6-b, which seems to indicate little disturbances of the jet certainly induced by small defaults of machining on the injection tube lip.

For a more detailed comparison, in Figure 7 is presented the radial profiles at different heights of the mean axial velocity sampled in the symmetrical plan of the turbulent jet. In the case without combustion (cf. Figure 7-a), the Gaussian shape of the velocity profiles in a free jet is clearly observable at the different heights, with the decrease of the axial velocity and the spreading of the profiles. For the 3 first heights in the case with combustion (cf. Figure 7-b), the same behaviour is observed. The resolution of the mean velocity is as good as than for the cold flow. The influence of the flame on the shape of the velocity profile becomes significant only in the upper part of the jet as shown in Figure 7-b from the velocity profile extracted at 42 mm to the injector. On that profile, the flame location is also clearly tagged by the steep variation of the velocity at 8 mm to the axial position. As in the Figure 6, the dissymmetry of the flame position is also observed.
In the present paper, the RMS profiles of the velocity have not been reported because the limited

number of instantaneous flow fields is not sufficient enough to ensure a statistical convergence of the results, especially in the case with combustion where the flame oscillations add fluctuating scales in the flow and so required larger dataset than in the case of cold flow. Nevertheless, to evaluate qualitatively the quality of velocity measurement, in Figure 8 are shown two examples of raw instantaneous 3D velocity fields. In both cases, the development of the jets seems well resolved and the continuity of the iso-surfaces suggests that the measurements are not too much affected by noise. From that volume representation is not easy to evaluate if the flame introduced any disturbance on the velocity measurement. In Figure 9 are presented four instantaneous velocity profiles for the axial (v) and radial (u) components at two different heights in the jet (20 and 40 mm). For the axial component, the raw instantaneous profiles in both cases are continuous without significant peak noise compared to the velocity range. In the case with combustion at 40 mm, the variability of the instantaneous flame position is shown by the random positioning of the steep variation to zero on the side of the profile. The low level of noise on the velocity measurements in both cases is confirmed on the profiles of the radial velocity component (cf. Figure 9). The velocity range of that component being around ten times smaller than the axial velocity component, it should be more sensitive than the axial component to the measuring noise. From our results, we can observe that in both cases, no random peak noise seems to affect significantly the continuity of the instantaneous measurement of the velocity profile of the radial jet velocity. From this qualitative comparison, it seems that the accuracy of the velocity measurement by tomo-PIV technique in the lifted-flame configuration is very comparable to the one obtained in the cold flow situation. And so, the influence of the unsteady variations of the refractive in an axisymmetric configuration is not affecting too much the reliability of the 3D velocity measurement.

5. Conclusion

In the present paper, an application of the tomographic PIV technique has been performed in a lifted-flame configuration in order to evaluate the influence of the unsteady variations of the refractive index induced by the flame brush and the burned gases regions. These results have been compared to those obtained in a free turbulent jet. The two flow configurations being investigated from the same optical arrangement, a qualitative comparison of results has been possible. From our analysis based on the comparison of the mean and instantaneous 3D velocity fields, no significant influence of the refractive index variation has been noted and the accuracy of measurement seems to be very comparable in both cases. We think that the tomo-PIV can be used with confidence in a simple axisymmetric flame configuration to investigate the interaction between large-scale turbulent structures and the flame.

In the future, two aspects seem to us important to investigate further in order to obtain more general conclusions concerning the use of the tomo-PIV to investigate reactive flows. First, it would be important to confirm our observations in a much more complex experimental configuration and also to analyse in more details the effect of the refractive index variation on the reconstructed volume itself by comparing for instance parameters as quality factors or the re-projected intensity profile of the volume. The second point concerns the reconstruction of the 3D flame surface from the tomo-PIV records. In the present paper, the flame surface location has been estimated from the velocity field, but in many combustion studies, the flame has to be localised with a much higher accuracy as it is currently performed in 2D from the PIV images [balusamy 2011]. Up to now, the too low particle density in the reconstructed volume pairs does not permit a straightforward extension of the flame extraction techniques developed in 2D and much more complex approaches has to be considered to access to the instantaneous 3D flame shape [Upton *et al* 2011]. The simultaneous measurement of the 3D flame structure and flow field from the same system is a very challenging aspect for the turbulent combustion.

Acknowledgement:

This work has been supported by the French National Agency (ANR) in the frame of the program: VIVE3D (ANR-07-1188-532) “Vélocimétrie Instantanée Volumique pour les Ecoulements Tridimensionnels".

References

Atkinson C., Soria J., (2009) An efficient simultaneous reconstruction technique for tomographic particle image velocimetry. Exp in Fluids 47: 553-568

Balusamy S., Cessou A. and Lecordier B. - Direct measurement of local instantaneous laminar burning velocity by a new PIV algorithm - Experiments in Fluids Volume 50, Number 4 (2011)

Cessou A., Varea, E., Criner, K., Godard G. and Vervisch, P. (2012)- Simultaneous measurements of OH, mixture fraction and velocity fields to investigate flame stabilization enhancement by electric field - Experiments in Fluids, Volume 52, Issue 4, pp.905-917

Eckbreth, A. C. - Laser Diagnostics for Combustion Temperature and Species, Combustion Science and Technology Book Series, Vol 3 - ISBN 0-85626-344-3 (1996)

Elsinga, G. E.; Scarano, F.; Wieneke, B. & van Oudheusden, B. W. (2006), 'Tomographic particle image velocimetry', Experiments in Fluids V41(6), 933--947.

Kohse-Hoeinghaus K., Barlow R.S., Alden M., Wolfrum J., “Combustion at the Focus: Laser Diagnostics and Control,” Proc. Combust. Inst. 30, 89-123, (2005)

Kohse-Höinghaus K., Jeffries J.B. (Eds.): Applied Combustion Diagnostics - Taylor Francis, New York 20.21 2002

Maurey C., Cessou A.; Lecordier B. & Stepowski D. (2000), Statistical flow dynamic properties conditioned on the oscillating stabilization location of turbulent lifted flame, *in* 'Symposium (International) on Combustion', Combustion Institute, Edinburgh, United Kingdom, pp. 545--551.

Novara M. and Scarano F. - Performances of motion tracking enhanced Tomo-PIV on turbulent shear flows - 5th Int Symp on Applications of Laser Techniques to Fluid Mechanics Lisbon, Portugal, 05-08 July, 2010

Su L.K., Sun O.S. & Mungal M.G. (2006) “Experimental Investigation of Stabilization Mechanisms in Turbulent, Lifted Jet Diffusion Flames,” *Comb. Flame* **144**, 494–512.

Thomas L., Tremblais B. and David L. - Influence des paramètres de reconstruction sur la qualité des résultats de tomo-PIV, Congrès Francophone de Techniques Laser, CFTL 2010, Vandoeuvre-lès-Nancy, 14-17 septembre 2010

Upton, T. D., Verhoeven D.D. and Hudgins E. - High-resolution computed tomography of a turbulent reacting flow - Exp Fluids (2011) 50:125–134 DOI 10.1007/s00348-010-0900-6

Wieneke, B. (2008), 'Volume self-calibration for 3D particle image velocimetry', Experiments in Fluids 45(4), 549--556.

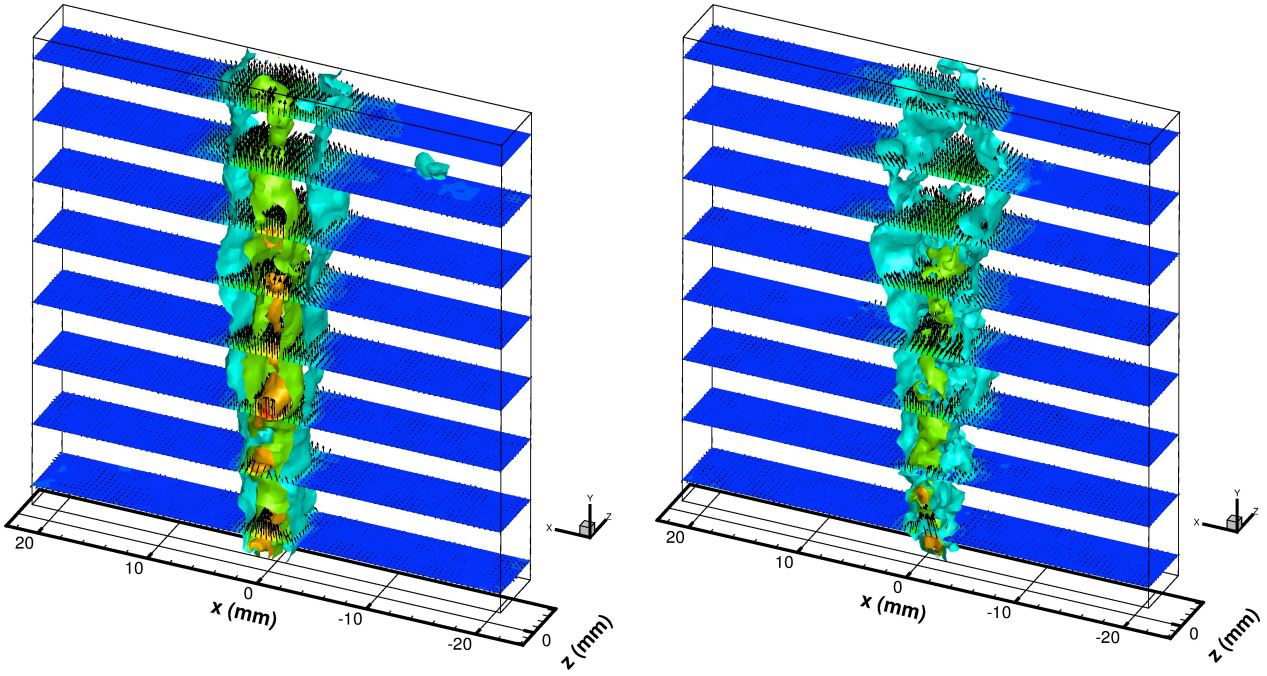

a) Cold flow **b) Hot flow**

Figure 8 – Example of raw instantaneous 3D velocity measurement of the cold and hot flows

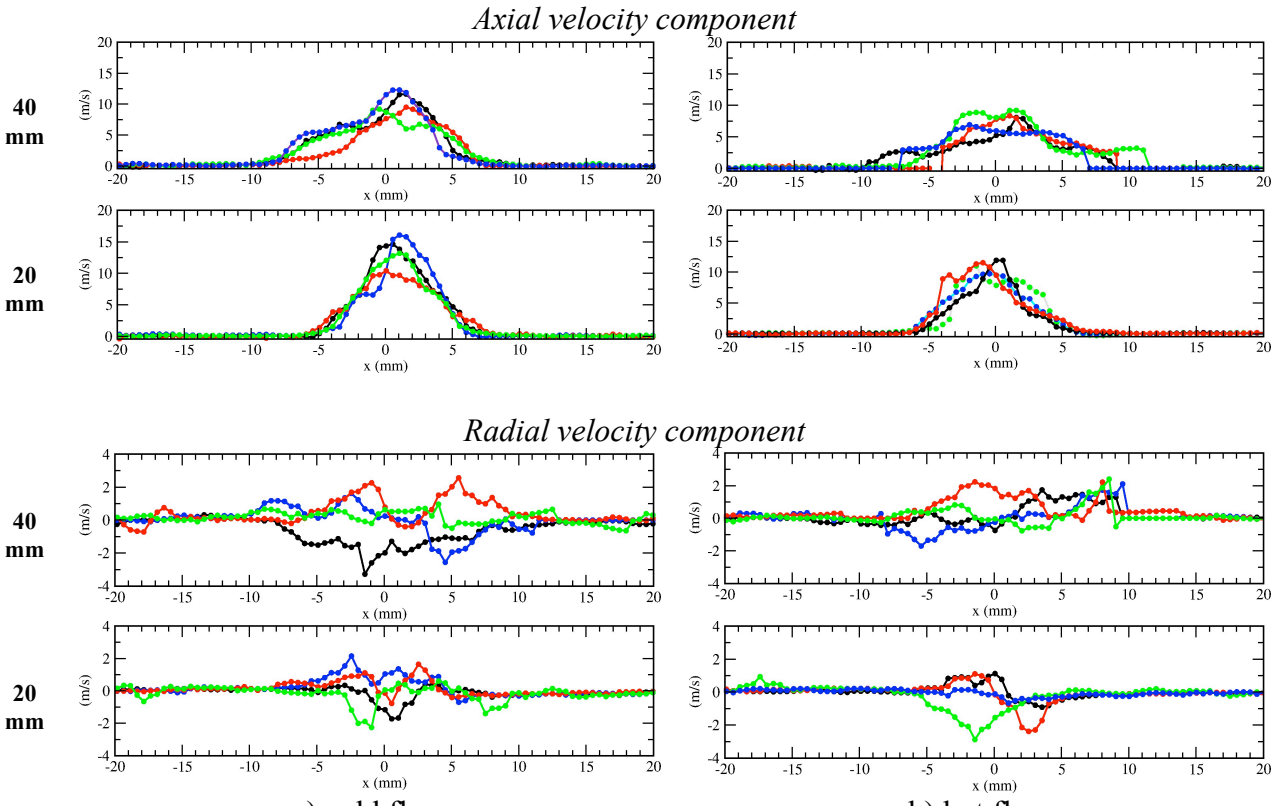

a) cold flow b) hot flow

Figure 9 – Four radial instantaneous velocity profiles of the velocity components u and v at two heights (20 and 40 mm)